

# Self-Supervised Cross-Modal Text-Image Time Series Retrieval in Remote Sensing

Genc Hoxha, *Member, IEEE*, Olivér Angyal and Begüm Demir, *Senior Member, IEEE*

**Abstract**—The development of image time series retrieval (ITSR) methods is a growing research interest in remote sensing (RS). Given a user-defined image time series (i.e., the query time series), the ITSR methods search and retrieve from large archives the image time series that have similar content to the query time series. The existing ITSR methods in RS are designed for unimodal retrieval problems, limiting their usability and versatility. To overcome this issue, as a first time in RS we introduce the task of cross-modal text-ITSR. In particular, we present a self-supervised cross-modal text-image time series retrieval (text-ITSR) method that enables the retrieval of image time series using text sentences as queries, and vice versa. In detail, we focus our attention on text-ITSR in pairs of images (i.e., bitemporal images). The proposed text-ITSR method consists of two key components: 1) modality-specific encoders to model the semantic content of bitemporal images and text sentences with discriminative features; and 2) modality-specific projection heads to align textual and image representations in a shared embedding space. To effectively model the temporal information within the bitemporal images, we introduce two fusion strategies: i) global feature fusion (GFF) strategy that combines global image features through simple yet effective operators; and ii) transformer-based feature fusion (TFF) strategy that leverages transformers for fine-grained temporal integration. Extensive experiments conducted on two benchmark RS archives demonstrate the effectiveness of the proposed method in accurately retrieving semantically relevant bitemporal images (or text sentences) to a query text sentence (or bitemporal image). The code of this work is publicly available at <https://git.tu-berlin.de/rsim/cross-modal-text-tsir>.

**Index Terms**—Text-image time series retrieval, self-supervised learning, bitemporal images, remote sensing.

## I. INTRODUCTION

The rapid advancements in remote sensing (RS) technology have resulted in an unprecedented growth of image archives that usually contain multitemporal images, i.e., images acquired over the same geographical area at different times. Accordingly, the development of content-based image time series retrieval (ITSR) methods that aim to query specific kinds of change relevant to the user from such archives has attracted great attention in RS. ITSR can be divided into two different categories: 1) retrieval of long-term changes; and 2) retrieval of short-term changes [1]. Examples of the former category include time-varying phenomena that can be observed at different time resolutions such as seasonal

changes. Retrieval of short-term changes, on the other hand, includes abrupt changes such as forest fires, floods, etc.

Any ITSR method essentially consists of (at least) two steps: 1) description of each image time series by a set of features; and 2) retrieval of time series of images similar to the query time series. Querying image time series from large RS data archives depends on the capability and effectiveness of the techniques in describing and representing the images [1], [2]. In the RS literature, several methods have been presented for ITSR purposes. As an example, Bovolo et al. [1] propose to exploit spectral change vector analysis to model the semantic content of bitemporal images and subsequently use the k-means clustering algorithm and Euclidean distance to perform bitemporal image retrieval, specifically for the retrieval of short-term changes. Ma et al. [3] employ several hand-crafted features based on color and texture to represent bitemporal images and performed retrieval by measuring the similarity between the query and archive bitemporal images in the feature space. However, hand-crafted features are unable to represent the rich semantic information contained in the image time series leading to limited retrieval performance. Deep neural networks (DNNs) have shown their effectiveness in learning discriminative image representations directly from raw images becoming a default selection for image representation learning in many RS applications [4], [5]. In the context of ITSR, Vuran et al. [2] investigate two methods based on DNNs to learn bitemporal image representations. The first method is based on deep change vector analysis [6] and consists of exploiting feature differences from different layers of convolution neural networks (CNNs). The second method is based on autoencoders and aims to reconstruct the difference image from the bitemporal images where the latent space of the autoencoder is used as bitemporal image representations. Retrieval is then performed by measuring the similarity of the query bitemporal images with the ones of the archive in the feature space [2].

The methods discussed above are designed for single-modality (i.e., unimodal) ITSR problems where query image time series and the archive are of the same modality. However, this unimodal setting imposes a significant limitation in operational scenarios as it assumes that users always have access to a query image time series example in the required modality. To overcome this limitation, enabling queries formulated in natural language (i.e., using text sentences) provides a more flexible and accessible alternative. Using text sentences as queries allows users to express complex spatial-temporal semantic concepts without requiring an exact image time series example. This significantly broadens the usability of ITSR systems in operational scenarios, making them more intuitive

Genc Hoxha and Begüm Demir are with the Faculty of Electrical Engineering and Computer Science, Technische Universität Berlin, 10623 Berlin, Germany and also with the Berlin Institute for the Foundations of Learning and Data (BIFOLD), 10623 Berlin, Germany (emails: genc.hoxha@tu-berlin.de, demir@tu-berlin.de).

Olivér Angyal is with the Faculty of Electrical Engineering and Computer Science, Technische Universität Berlin, 10623 Berlin, Germany (e-mail: oliver.angyal@gmail.com).

and adaptable to user needs.

In this paper, as a first time in RS, we introduce a novel and scientifically significant learning task that is cross-modal text-ITSR retrieval, where queries from one modality (e.g., text) can be matched to archive entries from another (e.g., image time series in RS). While text-image retrieval is widely studied for single-date images (see Section II), to the best of our knowledge, no prior work explored its extension to image time series in RS. The task of retrieving image time series based on natural language queries plays a critical role in effectively handling large-scale RS archives for searching long-term as well as short-term changes. We would like to note that text-ITSR is inherently more challenging than conventional text-image retrieval, since it requires to model the content of the image time series and to establish proper associations with the linguistic information presented in the temporal order. In this paper, as a solution to the text-ITSR problem, we introduce a self-supervised cross-modal text-ITSR method designed to retrieve relevant image time series using text sentences as queries and vice versa. Specifically, we devote our attention in the retrieval of short term changes and thus we consider pairs of bitemporal images and their text sentences. As shown in Fig. 1, the proposed text-ITSR method consists of two main modules: 1) modality-specific encoders (which extracts discriminative features from both text and bitemporal images; and 2) modality-specific projection heads (which learn a joint feature representation space between the bitemporal images and text sentences by employing the contrastive loss). To effectively model the semantic content of the bitemporal images, we introduce two main fusion strategies: i) global feature fusion (GFF) strategy that combines the global feature extracted from bitemporal images using two simple but effective operators, feature concatenation or element-wise feature subtraction and ii) transformer based feature fusion (TFF) that leverages the transformer architecture to combine the bitemporal information. Extensive experiments carried out on two RS benchmark archives composed of pairs of text and bitemporal images demonstrate the effectiveness of the proposed method for cross-modal text-bitemporal image retrieval.

The remaining part of this paper is organized as follows. Section II presents the related work on single-date text-image retrieval in RS. Section III introduces the proposed method. Section IV describes the considered RS image archives and the experimental setup, while the experimental results are presented in Section V. Finally, in Section VI, the conclusion of the work is drawn.

## II. RELATED WORK ON SINGLE-DATE TEXT-IMAGE RETRIEVAL IN RS

Our paper presents the first study in RS in the context of text-ITSR, whereas text-image retrieval (achieved on analyzing single-date images without considering temporal content) is widely investigated in RS. In detail, text-image retrieval aims at retrieving semantically relevant single-date RS images to a given user-defined query text, and vice versa [7]–[15]. Early works utilize image captioning systems to generate text

sentences of RS images and employ text matching techniques to perform the retrieval [7]. As an example, Hoxha et al. [7] propose a retrieval system that generates and exploits text sentences for text-image retrieval. Their approach utilizes an image captioning system as a combination of convolutional neural networks (CNNs) and long short-term memory (LSTM) [16] to generate text sentences of RS images, enabling the image-text retrieval based on text similarity. The resulting system allows users to perform image and text retrieval by utilizing either an image as a query (for which a text sentence is generated) or directly textual queries. However, this two-step approach heavily relies on the ability of the image captioning system in generating accurate captions of the query and archive images.

Recent advances in text-image retrieval systems in RS mainly focus on learning a joint image and text representation space, where images and their associated text are projected nearby each other [8]–[14]. In detail, modality-specific encoders are first used to represent images and text with discriminative features. These features are then further optimized and projected into the learned joint embedding space, where the retrieval is performed. The joint embedding space is learned through contrastive objectives such as pairwise contrastive loss [17] or triplet loss [18]. For example, Abdullah et al. [8] propose a deep bidirectional triplet network that consists of a CNN and an LSTM modality-specific encoder for image and text, respectively. They utilize triplet loss to learn a common embedding space, ensuring that semantically similar images and texts are projected close to each other, while dissimilar ones are placed farther apart. Similarly, CNNs and LSTMs are employed in [9] as image and text encoders where the common embedding space is learned in an unsupervised way through contrastive loss. A semantic alignment module is proposed in [10] that combines attention and gating techniques for a more representative joint embedding space. The attention mechanism is used to find and align image and textual correspondences, while the gating mechanism filters unnecessary information. Yuan et al. [19] present an asymmetric multimodal matching network that consists of a multi-scale visual self-attention module and a dynamic filtering function. The self-attention module captures multi-scale feature representations from RS images, while the dynamic filtering function removes redundant features. In a subsequent work [20], the authors refine their approach by introducing a lightweight multi-scale method optimized via knowledge distillation and contrastive loss enhancing the retrieval speed. In addition, Yuan et al. [21] also introduce a global-local information fusion module, which combines local features from a graph convolutional neural network (GCN) and global features from a CNN to generate multi-scale visual representations.

While the aforementioned methods rely on CNNs (pre-trained on ImageNet [22]) and recurrent neural networks (RNNs) as encoders for images and text, recent approaches have adopted Transformer-based models [23] as modality-specific encoders to enhance the text-image retrieval performances [12], [24]–[30]. This is mainly driven by leveraging the capabilities of the Contrastive Language-Image Pre-training (CLIP) foundation model [31]. As an example,

Rahhal et al. [12] propose a multi-language text-image retrieval approach that consists of pre-trained language and vision transformers (i.e., CLIP [31]) to extract text and image representations. Compared to previous works, their approach supports retrieval in multiple languages extending beyond English. Yuan et al. [24] propose a parameter-efficient transfer learning approach based on CLIP to effectively and efficiently transfer visual–language knowledge from the natural domain to the RS domain for text–image retrieval. Similarly, an uncertainty-aware prompt-learning approach is proposed in [25] to efficiently transfer the CLIP knowledge to RS domain. Hu et al. [26] propose a CLIP-based global-local information soft-alignment approach to align global and local image and text features utilizing pairwise contrastive loss. To obtain fine-grained features of local objects in the images, Wu et al [27] present a spatial-channel attention transformer with pseudo regions for text-image retrieval. The advantage of the method lies in automatically generating pseudo regions instead of utilizing object detectors to identify the objects present in the images. This is achieved by clustering semantically similar grid features using a clustering-based algorithm [32]. Each cluster represents a pseudo region from which local object features are extracted. Zhao et al. [28] introduce a masked interaction inferring and aligning (MIIA) module [28] that is integrated into CLIP to learn fine-grained image-text features. The MIIA module is a combination of self- and cross-attention modules to establish linkages between image and text representations by predicting masked image and text tokens.

Although the above-mentioned methods are effective for text-image retrieval in RS, they are not suitable for text-ITSR due to their inability to characterize the temporal content.

### III. PROPOSED METHOD

In this paper, we consider a self-supervised cross-modal text-ITSR problem. Let  $\mathcal{D} = \{(\mathbf{X}^i, \mathbf{Y}^i)\}_{i=1}^N$  be a multimodal training set consisting of  $N$  bitemporal images and text pairs. Let  $\mathbf{X}^i = (\mathbf{I}_{t_1}^i, \mathbf{I}_{t_2}^i)$  be the  $i^{\text{th}}$  pair of co-registered RS images acquired over the same geographical area at times  $t_1$  and  $t_2$ , respectively. Let  $\mathbf{Y}^i = (w_1, w_2, \dots, w_M)^i$  be the corresponding text sentence (with  $M$  ordered words  $w$ ) describing the changes between the co-registered images in  $\mathbf{X}^i$ . Given the multi-modal training set  $\mathcal{D}$ , the proposed self-supervised text-ITSR method aims to achieve cross-modal retrieval, where queries from one modality (e.g., text) can be matched to archive entries from another (e.g., image time series). The characterization of the semantic content of the bitemporal images and the text sentences with discriminative features is of great importance for an accurate text-ITSR system. To bridge the semantic gap between bitemporal images and text modalities, our method learns a joint representation space between text and bitemporal images where bitemporal images and text characterized by similar contents are projected nearby each other and vice versa. To this end, we represent bitemporal images and text with discriminative features through modality-specific encoders, followed by projecting and learning the joint representation (i.e., embedding) space. We utilize transformer architectures for both text and image modalities as specific

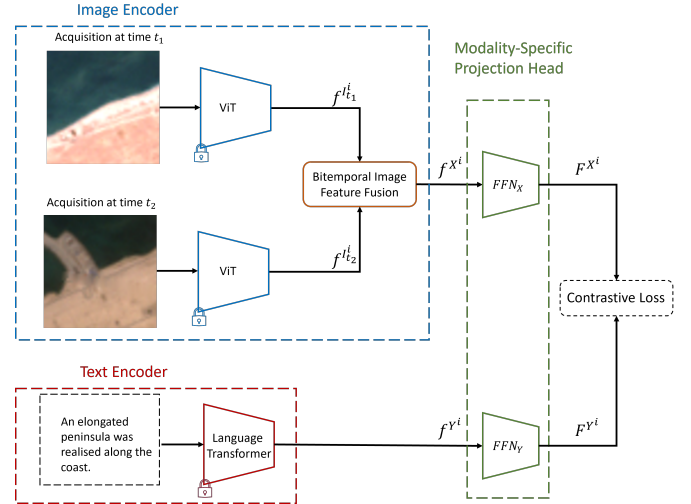


Fig. 1: Overall architecture of the proposed text-ITSR method.

encoders due to their proven capabilities in learning discriminative features.

Specifically, we use the bidirectional encoder representations from transformer (BERT) language model [33] as text encoder and the visual transformer (ViT) [34] as image encoder. The text features are obtained passing the input text sentence  $\mathbf{Y}^i$  through the pretrained BERT model as follows:

$$f^{Y^i} = BERT(\mathbf{Y}^i). \quad (1)$$

To obtain initial discriminative feature of the bitemporal images the ViT [34] consists of dividing an image  $I$  into non-overlapping patches which are then processed by a transformer encoder. The bitemporal image features are obtained passing the input bitemporal images  $\mathbf{I}_{t_1}^i, \mathbf{I}_{t_2}^i$  through the ViT encoder as follows:

$$f^{I_{t_1}^i} = ViT(\mathbf{I}_{t_1}^i) \quad (2)$$

$$f^{I_{t_2}^i} = ViT(\mathbf{I}_{t_2}^i) \quad (3)$$

To model the semantic content of the bitemporal images, we introduce two fusion strategies that are applied at the feature level (see Fig. 1). The first strategy considers the global features individually extracted from the ViT encoder and fuses them using two simple but effective operators, feature concatenation or element-wise feature subtraction. The second strategy is based on the transformer architecture and aims to better model the semantic content of bitemporal images by exploiting a cross-attention mechanism. After applying one of these fusion strategies, the resulting features of text sentences and bitemporal images are passed to their respective modality-specific projection heads. Contrastive learning is then utilized to align the features across modalities, enabling a robust joint representation space for cross-modal retrieval. In the following we provide a detailed description of our fusion strategies as well as the optimization of the proposed text-ITSR method.

#### A. Global Feature Fusion (GFF)

To achieve global feature fusion (GFF) we exploit the global features obtained by the class token embeddings in

the ViT. To this end, we present two simple but effective operators for GFF: 1) element-wise feature subtraction denoted as GFF: Subtraction; and 2) feature concatenation denoted as GFF: Concatenation. In detail, the GFF: Subtraction can be expressed as follows:

$$f^{\mathbf{X}^i} = f^{\mathbf{I}^{i_{t_2}}} - f^{\mathbf{I}^{i_{t_1}}} \quad (4)$$

whereas the GFF: Concatenation is defined as:

$$f^{\mathbf{X}^i} = \text{Concat}(f^{\mathbf{I}^{i_{t_2}}}, f^{\mathbf{I}^{i_{t_1}}}). \quad (5)$$

### B. Transformer-based Feature Fusion (TFF)

Instead of utilizing global image features that are obtained from the class token embeddings in the ViT, the TFF strategy utilizes directly the patch embedding of bitemporal images in  $X_i$ . Accordingly, it processes and fuses through multiple stages the patch embedding  $f^{\mathbf{I}^{i_{t_2}}}, f^{\mathbf{I}^{i_{t_1}}} \in \mathbb{R}^{T \times d_{E_I}}$  obtained from the bitemporal images. Fig. 2 shows an illustration of the TFF strategy that is mainly based on [35] with some adaptation to the ViT image encoder. With the aim of modeling the changes between bitemporal images, the first step of the TFF consists of taking the difference between patch embeddings

$$s^{\mathbf{X}^i} = f^{\mathbf{I}^{i_{t_2}}} - f^{\mathbf{I}^{i_{t_1}}} \quad s^{\mathbf{X}^i} \in \mathbb{R}^{T \times d_{E_I}} \quad (6)$$

where  $T$  and  $d_{E_I}$  are the total number of patches and the patch embedding dimensions, respectively. To better extract and exploit the correlation between the patch embeddings, the difference of the patch embeddings is passed through a cross-attention layer:

$$\text{CrossAttention}(Q, K, V) = \text{softmax}\left(\frac{QK^T}{\sqrt{d}}\right)V \quad (7)$$

where the image pair patch embeddings  $f^{\mathbf{I}^{i_{t_1}}}, f^{\mathbf{I}^{i_{t_2}}} \in \mathbb{R}^{T \times d_{E_I}}$  serve as query  $Q$ , their difference  $s^{\mathbf{X}^i} \in \mathbb{R}^{T \times d_{E_I}}$  vector as key  $K$  and value  $V$ . With the scaled dot product of  $Q$  and  $K$ , an attention score is calculated between each pair of vectors in the input sequence. Intuitively, this is a measure of similarity, that is, how relevant the query vector is to the key vector. The scaling by  $\sqrt{d}$  ( $d$  being the internal hidden dimension) is a normalization factor that tends to make training more stable [23]. Through the softmax function, normalized attention scores are obtained for each vector. Finally, multiplying the normalized attention scores with  $V$  produces the context-aware representation of each vector.

As in the standard transformer architecture [23], the above process is repeated  $n$  times to allow the model to pay attention to the input from different aspects. To this end, the cross-attention mechanism defined in (7) is performed  $n$  times, with each attention head having its own set of learnable weight matrices. Thus, queries, keys, values and the final representation will differ for each head. The outputs of the attention heads are concatenated and multiplied with a separate learnable weight matrix  $W^O \in \mathbb{R}^{nd \times d_{E_I}}$  in order to match the input dimensions of the next layer as described in (8) and (9)

$$\text{MultiHead}(f^{\mathbf{I}^{i_{t_2}}}, f^{\mathbf{I}^{i_{t_1}}}, s^{\mathbf{X}^i}) = \text{Concat}(\text{head}_1, \dots, \text{head}_n)W^O \quad (8)$$

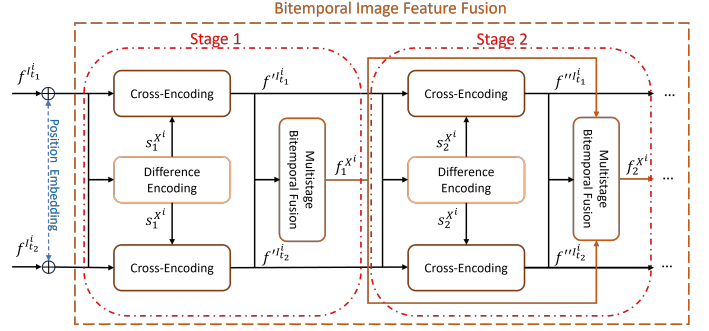


Fig. 2: Architecture of the feature fusion of bitemporal images.

$$\text{head}_k = \text{CrossAttention}(f^{\mathbf{I}^{i_{1,2}}} W_k^Q, s^{\mathbf{X}^i} W_k^K, s^{\mathbf{X}^i} W_k^V) \quad (9)$$

where  $W_k^Q, W_k^K, W_k^V \in \mathbb{R}^{d_{E_I} \times d}$  are the learnable matrices of the  $k^{\text{th}}$  head and  $f^{\mathbf{I}^{i_{1,2}}}$  represents the bitemporal features in a compact manner. Following [35], the output of the MultiHead attention mechanism is added to the original bitemporal patch embedding  $f^{\mathbf{I}^{i_{1,2}}} \in \mathbb{R}^{T \times d_{E_I}}$

$$f^{\mathbf{I}'_{1,2}} = \text{LN}(f^{\mathbf{I}^{i_{1,2}}} + \text{MultiHead}(f^{\mathbf{I}^{i_{1,2}}})) \quad (10)$$

$$f^{\mathbf{I}''_{1,2}} = \text{LN}(f^{\mathbf{I}'_{1,2}} + g(f^{\mathbf{I}'_{1,2}})) \quad (11)$$

where  $g(\cdot)$  represents two fully connected layers with RELU activation function, respectively. The bitemporal features  $f^{\mathbf{I}''_{1,2}}$  (i.e.,  $f^{\mathbf{I}''_{t_1}}$  and  $f^{\mathbf{I}''_{t_2}}$ ) obtained utilizing (11) are then fused together through multiple fusion stages as depicted in Fig. 2. A single fusion stage can be described by the following equation:

$$f_l^{\mathbf{X}^i} = \text{LN}(\text{Concat}(f^{\mathbf{I}''_{t_1}}, f^{\mathbf{I}''_{t_2}}) + f_{l-1}^{\mathbf{X}^i} + r(\text{Concat}(f^{\mathbf{I}''_{t_1}}, f^{\mathbf{I}''_{t_2}}) + f_{l-1}^{\mathbf{X}^i})) \quad (12)$$

where  $f_{l-1}^{\mathbf{X}^i} \in \mathbb{R}^{T \times 2d}$  represents the output of the  $l-1$  fusion stage,  $r(\cdot)$  a residual block of three convolutional layers, batch normalization and drop out layers [35].

### C. Network optimization

Once the fused bitemporal images and text embeddings are obtained, they are given as input to the respective modality-specific projection heads (see Fig. 1) that consist of feed-forward neural networks (FFN). The aim of the modality-specific projection heads is to map the fused bitemporal images and text representations to a fixed length-vector as follows:

$$F^{\mathbf{X}^i} = \text{FNN}_X(f^{\mathbf{X}^i}) \quad (13)$$

$$F^{\mathbf{Y}^i} = \text{FNN}_Y(f^{\mathbf{Y}^i}) \quad (14)$$

where  $F^{\mathbf{X}^i} \in \mathbb{R}^{1 \times d_F}$  and  $F^{\mathbf{Y}^i} \in \mathbb{R}^{1 \times d_F}$  are the mapped image and text representations, respectively and  $d_F$  represents their dimensionality. To learn the joint embedding space of text and bitemporal images, we employ the contrastive loss described by Radford et al. [31], due to its effectiveness in



jointly learning and aligning image and text representations. In detail, let  $B = \{\mathbf{X}^i, \mathbf{Y}^i\}_{i=1}^b$  represent a mini-batch of size  $b$  randomly sampled from the training set  $\mathcal{D}$ . Passing this mini-batch as input to the proposed model produces the following bitemporal images and text representations  $\{F^{\mathbf{X}^i}\}_{i=1}^b$  and  $\{F^{\mathbf{Y}^i}\}_{i=1}^b$ , respectively. The learning objective is to maximize the similarity of  $b$  correct bitemporal images and text pairs, while minimizing the similarity between  $b^2 - b$  incorrect pairs within the mini-batch [31]. To this end, the loss is computed in both the image and text domains. In the image domain, the objective is to bring the text features closer to their corresponding image features, while pushing them away from other text features within the mini-batch. Similarly, in the text domain, the aim is to bring the corresponding image features closer, while pushing away the other image features within the mini-batch. This is achieved through the bidirectional normalized temperature-scaled cross-entropy losses defined as follows [36]:

$$L_{F^{\mathbf{X}} \rightarrow F^{\mathbf{Y}}} = -\frac{1}{b} \sum_{i=1}^b \log \frac{\exp(\cos(F^{\mathbf{X}^i}, F^{\mathbf{Y}^i}) \exp(\kappa))}{\sum_{j=1}^b \exp(\cos(F^{\mathbf{X}^i}, F^{\mathbf{Y}^j}) \exp(\kappa))} \quad (15)$$

$$L_{F^{\mathbf{Y}} \rightarrow F^{\mathbf{X}}} = -\frac{1}{b} \sum_{i=1}^b \log \frac{\exp(\cos(F^{\mathbf{Y}^i}, F^{\mathbf{X}^i}) \exp(\kappa))}{\sum_{j=1}^b \exp(\cos(F^{\mathbf{Y}^i}, F^{\mathbf{X}^j}) \exp(\kappa))} \quad (16)$$

where  $\kappa$  is a learnable temperature parameter that controls the sharpness of the distribution and  $\cos(\cdot)$  is the cosine similarity. To account for both contributions, the final loss is the average of the two loss terms:

$$L_C = \frac{1}{2}(L_{F^{\mathbf{X}} \rightarrow F^{\mathbf{Y}}} + L_{F^{\mathbf{Y}} \rightarrow F^{\mathbf{X}}}). \quad (17)$$

After training, we obtain the features of bitemporal images and text sentences as the output of the respective modality-specific projection heads. The obtained features are then stored in the feature archive for the cross-modal retrieval. Then, to retrieve semantically similar bitemporal images to a query provided as a text sentence  $\mathbf{Y}^q$ , we compute the cosine similarity between the  $FNN_Y(f^{\mathbf{Y}^q})$  and the bitemporal image features in the archive. The distances are ranked in ascending order, and the top- $k$  bitemporal images are retrieved. Similarly, when the query is provided as a bitemporal image  $\mathbf{Y}^q$ , the cosine similarity between  $FNN_X(f^{\mathbf{X}^q})$  and the feature in the retrieval archive are computed, ranked and the  $k$  text sentences are retrieved.

## IV. DATASET DESCRIPTION AND EXPERIMENTAL DESIGN

### A. Datasets

To assess the performance of the proposed method, we carried out our experiments on two benchmark archives.

The first archive, LEVIR Change Captioning (LEVIR-CC) [35] comprises 10077 RGB image pairs of size  $256 \times 256$  pixels with a spatial resolution of 0.5 meters. The image pairs within the LEVIR-CC dataset predominantly consider building-related changes in the area of Texas, USA. The acquisition time spans from 2002 to 2018, with a minimum of 5 and a maximum of 14 years between the acquisition of the

two images of each pair. Each image pair is annotated with 5 different change descriptions. Notably, half of the dataset contains scenes depicting no change between the two images. In such case, all the image pairs are annotated with the same set of 5 change captions.

The second archive, Dubai Change Captioning Dataset (Dubai CCD) [37] considers the urban development of the city of Dubai. It comprises 500 multispectral image pairs acquired by Enhanced Thematic Mapper Plus (ETM+) sensor onboard Landsat 7. Each image pair captures a 10-year span, with the first image acquired on May 19, 2000 and the second on June 16, 2010. The bitemporal images are of size  $50 \times 50$  pixels and contain 6 bands (i.e., R,G,B, near-infrared, short-wave infrared and mid-infrared) each of which is characterized by a spatial resolution of 30 meters. Each image pair is annotated with 5 different captions by expert annotators. Unlike the first archive, image pairs depicting no change are not always described by the same five captions. In such case, various captions are provided, introducing variability even when there is no semantic difference between the images.

### B. Experimental Setup

In our experiments, we used the predefined dataset splits to assess the performance of the proposed method. For the Dubai CCD the splits are as follows: 60%, 10%, and 30% for training, validation and testing, respectively. The splits for the LEVIR-CC dataset are 80% for training, 10% for validation, and 10% for testing. Each caption is paired with its corresponding bitemporal image pair separately. To stabilize training for the LEVIR-CC dataset, we used only 15% of the text and bitemporal image pairs that depict no changes. This decision was due to the dataset composition, where half of the samples represent no-change scenes annotated with the same set of five change descriptions. For evaluation, we merged the test and validation splits employing a leave-one-out strategy where one example is used as the query and the rest is used as the archive. The evaluation is repeated five times, each time selecting a random caption for every image pair at each time. The final results are averaged across all rounds. The evaluation is done considering two retrieval tasks: 1)  $T \rightarrow I$  is the task where the query is the text modality and the retrieval is applied to an archive of bitemporal images; and 2)  $I \rightarrow T$  where the query is the image modality (i.e., bitemporal images) and the retrieval is applied to an archive of text sentences. We utilized the pre-trained CLIP's Vision Transformer (ViT-B/16) as image encoder [31]. In the TFF strategy we used a total of three fusion stages (i.e.,  $l = 3$ ) and the patch embeddings as image representations. For the GFF strategies, we used the class token embedding as global features to represent the bitemporal images. We used CLIP's pre-trained text encoder and the class token embeddings to represent the text sentences [31]. Both scaled and channel-wise normalized images are passed through the respective backbone networks before applying the fusion methods.

The modal-specific feed-forward neural networks used in the projection heads consist of a hidden layer with 256 dimensions using ReLU activations and an output layer (i.e.,

$d_X, d_Y$ ) with 128 dimensions. The networks have a learnable temperature parameter  $\kappa$  that is initialized to 0.07 as suggested in [31]. For optimization, we used mini-batch stochastic gradient descent (SGD) with a batch size of 32, a learning rate of 0.01, weight decay of  $5 \times 10^{-4}$ , and momentum of 0.9. The models are trained for 30 epochs on NVIDIA A100 GPUs.

### C. Evaluation Metrics

We measured the retrieval performance using bilingual evaluation understudy (BLEU) [38], metric for evaluation of translation with explicit ordering (METEOR) [39] and recall-oriented understudy for Gisting evaluation (ROUGE-L) [40], for both  $T \rightarrow I$  and  $I \rightarrow T$  retrieval tasks. It is worth noting that the aforementioned metrics are commonly used in machine translation and in image captioning to measure the similarity between generated sentence descriptions (i.e., hypothesis) and the reference sentence descriptions. To this end, BLEU score measures the  $n$ -gram (i.e.,  $n$ -consecutive words) precision to quantify the similarity between the hypotheses and reference descriptions, where  $n = 1, 4$  in this work. ROUGE-L is based on the calculation of the F-score with respect to the longest common subsequence between the hypothesis and the reference descriptions. Finally, METEOR computes the weighted F-score, with more weight given to the recall and considers semantic similarity of the words (i.e., synonyms). All the used metrics range from 0 to 1, where a score of 1 indicates a perfect match.

To apply these metrics to our retrieval tasks, we appropriately defined the hypotheses and references. For the text-to-bitemporal image retrieval task (i.e.,  $T \rightarrow I$ ), the query text is treated as the hypothesis, while the reference captions of the retrieved bitemporal images served as references. In the bitemporal image-to-text retrieval task (i.e.,  $I \rightarrow T$ ), the five captions associated with the query bitemporal images are used as references, while the retrieved captions are considered as the hypothesis. This adaptation ensures consistent and fair evaluation in both retrieval tasks. We measure the retrieval performance using the aforementioned metrics on the top five retrieved data for each query. For a given query text or bitemporal images, the scores are computed individually for each retrieved data (i.e., bitemporal images or text) and then averaged. Finally, the overall performance is obtained averaging the scores for all the available queries.

## V. EXPERIMENTAL RESULTS

In this section, we present the results of the proposed text-ITSR method with its different fusion strategies applied to two retrieval tasks: 1)  $T \rightarrow I$ ; and 2)  $I \rightarrow T$  under three distinct scenarios: 1) full query set scenario (which includes queries, either text sentences or bitemporal images, that are associated to change and no change); 2) change query set scenario (which includes only those queries associated to change); and 3) no-change query set scenario (which includes only those textual or bitemporal images queries that are associated to no change). We would like to note that since, according to our knowledge, our method is the first study on text-ITSR in RS, there is no method available for direct comparison with it.

### A. Experimental Results on Levir CC

In this subsection we present the retrieval results of the proposed text-ITSR method on the LEVIR CC dataset. Table I reports the retrieval performances of the proposed method under different fusion strategies, tasks and scenarios.

1) *Full query set scenario*: In this scenario, the proposed text-ITSR method achieves the highest retrieval performance for both  $T \rightarrow I$  and  $I \rightarrow T$  retrieval tasks when employing the TFF strategy to model the semantic content of bitemporal images. Specifically, for the  $T \rightarrow I$  retrieval task, the proposed method achieves a BLEU-4 score of 0.568 using the TFF strategy, that is 13% and 8% higher compared to employing GFF: Subtraction and GFF: Concatenation strategies, respectively. In other words, the reference sentence descriptions of bitemporal images retrieved by the proposed text-ITSR method when utilizing the TFF strategy contain the highest number of overlapping 4-grams (i.e., 4 consecutive words) with the query sentence description. This indicates that the retrieved bitemporal images utilizing the TFF strategy in the proposed method are highly correlated with the query sentence description. This superior performance of the proposed method with TFF strategy is further confirmed by looking at the achieved scores in terms of METEOR and ROUGE-L.

For instance, the proposed method achieves a METEOR score of 0.565 with the TFF strategy, which is 21% and 16% higher than the scores achieved with the GFF: Subtraction and GFF: Concatenation strategies, respectively. Similarly, a ROUGE-L score of 0.695 is obtained when using the TFF strategy, representing an improvement of 12% and 8% over the utilization of the GFF: Subtraction and GFF concatenation strategies, respectively.

These METEOR and ROUGE-L scores indicate that the retrieved bitemporal images by the proposed text-ITSR method are associated with reference sentences that exhibit greater lexical and semantic similarity to the query description when using the TFF strategy compared to those retrieved using the GFF strategies. This consistency across metrics highlights the robustness of TFF strategy in effectively modeling the semantic content of the bitemporal images. Consequently, integrating the TFF strategy into the proposed text-ITSR method significantly enhances its ability to retrieve semantically aligned bitemporal images for query sentence descriptions, outperforming the GFF strategies.

A similar behavior can be observed for the  $I \rightarrow T$  retrieval task where using the TFF strategy the proposed text-ITSR method achieves the highest retrieval results across all the metrics. With the TFF strategy the proposed method achieves a BLEU-4 score of 0.477, which is approximately 16% and 14% higher compared to employing GFF: Subtraction and GFF: Concatenation strategies, respectively. This indicates that the retrieved text sentences using the TFF strategy contain a higher overlap of words with the reference descriptions of the query bitemporal images compared to those retrieved with the GFF strategies. This shows the superiority of the TFF strategy in retrieving text sentences that are relevant to the query bitemporal images. This behavior is also confirmed by the METEOR and ROUGE-L scores where using the TFF

TABLE I: BLEU-1, BLEU-4, METEOR, and ROUGE-L results on text-to-bitemporal images ( $T \rightarrow I$ ), bitemporal image-to-text ( $I \rightarrow T$ ) retrieval tasks and the average across the two retrieval tasks of the proposed fusion strategies for the LEVIR-CC dataset using full, change and no-change query sets.

Query Set: Full												
Fusion Strategy	BLEU-1			BLEU-4			METEOR			ROUGE-L		
	$I \rightarrow T$	$T \rightarrow I$	Average	$I \rightarrow T$	$T \rightarrow I$	Average	$I \rightarrow T$	$T \rightarrow I$	Average	$I \rightarrow T$	$T \rightarrow I$	Average
GFF: Concatenation	0.597	0.698	0.647	0.331	0.487	0.409	0.388	0.407	0.397	0.512	0.616	0.564
GFF: Subtraction	0.577	0.648	0.612	0.313	0.434	0.373	0.362	0.355	0.358	0.492	0.575	0.534
<b>TFF</b>	<b>0.712</b>	<b>0.775</b>	<b>0.744</b>	<b>0.477</b>	<b>0.568</b>	<b>0.523</b>	<b>0.515</b>	<b>0.565</b>	<b>0.540</b>	<b>0.625</b>	<b>0.695</b>	<b>0.660</b>

Query Set: Change												
Fusion Strategy	BLEU-1			BLEU-4			METEOR			ROUGE-L		
	$I \rightarrow T$	$T \rightarrow I$	Average	$I \rightarrow T$	$T \rightarrow I$	Average	$I \rightarrow T$	$T \rightarrow I$	Average	$I \rightarrow T$	$T \rightarrow I$	Average
GFF: Concatenation	0.594	0.576	0.585	0.166	0.169	0.167	0.235	0.232	0.233	0.423	0.416	0.420
GFF: Subtraction	0.591	0.538	0.564	0.166	0.147	0.156	0.232	0.219	0.225	0.420	0.393	0.406
<b>TFF</b>	<b>0.613</b>	<b>0.600</b>	<b>0.607</b>	<b>0.189</b>	<b>0.186</b>	<b>0.187</b>	<b>0.242</b>	<b>0.241</b>	<b>0.242</b>	<b>0.438</b>	<b>0.432</b>	<b>0.435</b>

Query Set: No-change												
Fusion Strategy	BLEU-1			BLEU-4			METEOR			ROUGE-L		
	$I \rightarrow T$	$T \rightarrow I$	Average	$I \rightarrow T$	$T \rightarrow I$	Average	$I \rightarrow T$	$T \rightarrow I$	Average	$I \rightarrow T$	$T \rightarrow I$	Average
GFF: Concatenation	0.600	0.820	0.710	0.496	0.805	0.651	0.541	0.582	0.562	0.602	0.815	0.708
GFF: Subtraction	0.563	0.757	0.660	0.459	0.721	0.590	0.491	0.491	0.491	0.565	0.757	0.661
<b>TFF</b>	<b>0.811</b>	<b>0.951</b>	<b>0.881</b>	<b>0.765</b>	<b>0.951</b>	<b>0.858</b>	<b>0.787</b>	<b>0.889</b>	<b>0.838</b>	<b>0.812</b>	<b>0.959</b>	<b>0.885</b>

strategy the proposed method achieves highest retrieval results, demonstrating its superiority in the  $I \rightarrow T$  retrieval task.

Table I also presents the average performance of the proposed method across both retrieval tasks. Here, the utilization of the TFF strategy in the proposed text-ITSR method again demonstrates superior retrieval accuracy, achieving the highest retrieval scores across BLEU-4, METEOR, and ROUGE-L metrics.

2) *Change query set scenario:* In line with the previous scenario, one can notice that when the TFF strategy is used to model the semantic content of the bitemporal images, the proposed method achieves the highest retrieval scores across all the metrics and over the two retrieval tasks. For the  $T \rightarrow I$  retrieval task, one can see that with the TFF strategy the proposed method achieves a BLEU-4 score of 0.186, surpassing the utilization of the GFF: Subtraction and GFF: Concatenation strategies by approximately 4% and 2%, respectively. We can see that this behavior is also true for the METEOR and ROUGE-L metrics. For instance, in terms of ROUGE-L, with the TFF strategy the proposed method achieves a score of 0.432, improving over the utilization of GFF: Subtraction and GFF: Concatenation strategies by approximately 4% and 2%, respectively. The utilization of the TFF strategy in the proposed method also leads to higher

METEOR scores compared to the GFF strategies, showing its ability in retrieving bitemporal images that are characterized by similar changes as the query change descriptions. This higher performance is due to the TFF’s capability on learning discriminative features that highlight bitemporal differences, which is crucial for accurately retrieving bitemporal images that align with change-specific text sentences.

For the  $I \rightarrow T$  retrieval task, we can similarly observe that with the TFF strategy the proposed method continues to achieve higher results compared to the utilization of the GFF strategies. For instance, with the TFF strategy the proposed method achieves a BLEU-4 score of 0.189, outperforming the utilization of the GFF: Subtraction and GFF: Concatenation strategies by 3.3%. Similarly, METEOR and ROUGE-L metrics further demonstrate TFF’s strong performance in the  $I \rightarrow T$  retrieval task. These results emphasize the robustness of the TFF in handling changed-focused queries across modalities, thanks to its capabilities to explicitly model bitemporal images semantic content. This is further observed by analyzing the average scores across both of the retrieval tasks where the TFF strategy clearly outperforms the GFF strategies.

3) *No-change query set scenario:* For the task of retrieving bitemporal images where the queries are text sentences ( $T \rightarrow I$ ) in the no change query set scenario, the utilization of the



Fig. 3:  $T \rightarrow I$  retrieval example for Levir CC. a) query text and retrieved bitemporal images by the proposed cross-modal text-ITSR method when the: b) GFF: Concatenation, c) GFF: Subtraction and d) TFF strategies are used to model the semantic content of bitemporal images.

TFF strategy continue to dominate, by achieving the highest scores across all metrics and outperforming the the utilization of the GFF strategies by a significant margin. Specifically, with the TFF strategy the proposed method achieves a score of 0.951, significantly outperforming the utilization of the GFF strategies by approximately 23%, 15%, in terms of BLEU-4 score. Similar behavior can also be observed by looking and the achieved METEOR and ROUGE-L scores.

Similarly, for the  $I \rightarrow T$  retrieval task, we can see that the utilization of the TFF strategy in the proposed text-ITSR method outperforms the GFF strategies across all the metrics. As an example, with the TFF strategy the proposed method achieves a BLEU-4 score of 0.765, significantly outperforming the utilization of the GFF: Subtraction and Concatenation strategies by approximately 23% and 27%, respectively. We can see a similar behavior in terms of METEOR and ROUGE-L scores, showing the high capability of the proposed method with TFF strategy in retrieving no change text sentences with respect to a query bitemporal images that do not show change. Looking at the average scores across both retrieval tasks, one can see that in terms of BLEU-4 and ROUGE-L, the utilization of the TFF strategy outperforms the utilization of the GFF strategies, again showing a better performance on both retrieval tasks, similar to the other query set scenarios.

Fig. 3 shows a  $T \rightarrow I$  retrieval example where the query text is: "A row of houses are built along the road." and the

bitemporal images retrieved by the proposed cross-modal text-ITSR method using the GFF: Concatenation [Fig. 3 b)], GFF: Subtraction [see Fig. 3 c)] and TFF [see Fig. 3 d)] strategies to model the semantic content of the bitemporal images. First, one can notice that almost the retrieved bitemporal images depict changes involving the construction of rows of houses on the sides of the road. However, upon closer examination, the retrieved images obtained when using the TFF strategy in the proposed method exhibit a stronger alignment with the query text compared to those retrieved when using the GFF strategies. Specifically, with the TFF strategy [Fig. 3(d)], all the retrieved bitemporal images represent changes involving the construction of a row of houses along the road. In contrast, while with the GFF strategies the proposed method retrieves images depicting general construction activities along a road, they mostly fail to retrieve images that strictly conform to the "a single row of houses" criterion. For instance, with the GFF: Subtraction strategy the proposed method only two out of five retrieved images ( $2^{nd}$  and  $4^{th}$ ) depict the exact construction of a row of houses along a road. Another observation is that with the GFF: Subtraction strategy the  $5^{th}$  retrieved image does not even depict changes over the two acquisitions. With the GFF: Concatenation strategy, the proposed method retrieves more relevant images to the query text sentences compared to the GFF: Subtraction. As we can see from the retrieved images in Fig. 3 b) two out of the five retrieved images do not exactly align with the query text sentence. For instance, the  $2^{nd}$  and  $3^{rd}$  retrieved images depict the addition of a building in an existing residential area and the construction of two rows of houses along a road, respectively. These qualitative observations highlight the superiority of the TFF strategy in effectively modeling the changes within bitemporal images compared to the GFF strategies. Consequently, the use of the TFF strategy in the proposed text-ITSR method achieves better alignment between the textual and image modalities, leading to more accurate  $T \rightarrow I$  retrieval results.

Fig. 4 shows an  $I \rightarrow T$  retrieval example where one of the reference descriptions of the query bitemporal images [Fig. 4 a)] is "The woods have turned into roads with houses built alongside." and the text sentences retrieved by proposed cross-modal text-ITSR method using the GFF: Concatenation [Fig. 4 b)], GFF: Subtraction [see Fig. 4 c)] and TFF [see Fig. 4 d)] strategies to model the semantic content of the bitemporal images. One can see that almost all the retrieved text sentences semantically correspond to the change between the two image acquisitions: the disappearance of a forest area and the appearance of buildings alongside the roads. One can notice that using TFF, the retrieved text sentences by the proposed method are more aligned with the query bitemporal images compared to the utilization of the GFF strategies. In particular, one can notice that all of them describe the complete deforestation of the area and its replacement with roads and buildings. In contrast, the retrieval results obtained by utilizing the GFF strategies contain some inaccuracies, highlighted in red in [Fig. 4]. For example, the first retrieved text sentence by the proposed method with the GFF: Concatenation strategy describe that most of the trees have been removed and are replaced by massive houses. However, the query bitemporal





TABLE II: BLEU-1, BLEU-4, METEOR and ROUGE-L results on text-to-bitemporal images ( $T \rightarrow I$ ), bitemporal image-to-text ( $I \rightarrow T$ ) retrieval tasks and the average across the two retrieval tasks of the proposed fusion strategies for the DUBAI-CCD dataset on full, change and no-change query sets.

Query Set: Full												
Fusion Strategy	BLEU-1			BLEU-4			METEOR			ROUGE-L		
	$I \rightarrow T$	$T \rightarrow I$	Average	$I \rightarrow T$	$T \rightarrow I$	Average	$I \rightarrow T$	$T \rightarrow I$	Average	$I \rightarrow T$	$T \rightarrow I$	Average
GFF: Concatenation	0.554	0.514	0.534	0.232	0.210	0.221	0.301	0.265	0.283	0.480	0.504	0.492
GFF: Subtraction	0.571	<b>0.607</b>	0.589	0.205	0.280	0.242	0.309	<b>0.322</b>	0.321	0.485	<b>0.551</b>	0.518
TFF	<b>0.604</b>	<b>0.607</b>	<b>0.605</b>	<b>0.262</b>	<b>0.282</b>	<b>0.272</b>	<b>0.332</b>	0.312	<b>0.322</b>	<b>0.523</b>	0.537	<b>0.530</b>
Query Set: Change												
Fusion Strategy	BLEU-1			BLEU-4			METEOR			ROUGE-L		
	$I \rightarrow T$	$T \rightarrow I$	Average	$I \rightarrow T$	$T \rightarrow I$	Average	$I \rightarrow T$	$T \rightarrow I$	Average	$I \rightarrow T$	$T \rightarrow I$	Average
GFF: Concatenation	<b>0.562</b>	0.520	0.541	<b>0.208</b>	0.165	0.187	<b>0.274</b>	0.245	0.260	<b>0.471</b>	0.435	0.453
GFF: Subtraction	0.526	0.560	0.543	0.186	0.201	0.193	0.243	0.274	0.259	0.432	0.471	0.452
TFF	0.553	<b>0.575</b>	<b>0.564</b>	0.195	<b>0.224</b>	<b>0.210</b>	0.255	<b>0.295</b>	<b>0.275</b>	0.460	<b>0.488</b>	<b>0.474</b>
Query Set: No-change												
Fusion Strategy	BLEU-1			BLEU-4			METEOR			ROUGE-L		
	$I \rightarrow T$	$T \rightarrow I$	Average	$I \rightarrow T$	$T \rightarrow I$	Average	$I \rightarrow T$	$T \rightarrow I$	Average	$I \rightarrow T$	$T \rightarrow I$	Average
GFF: Concatenation	0.541	0.505	0.523	0.272	0.289	0.281	0.347	0.300	0.323	0.496	0.622	0.559
GFF: Subtraction	0.651	<b>0.687</b>	0.669	0.236	<b>0.419</b>	0.328	0.423	<b>0.433</b>	<b>0.428</b>	0.577	<b>0.689</b>	<b>0.633</b>
TFF	<b>0.692</b>	0.662	<b>0.677</b>	<b>0.378</b>	0.382	<b>0.380</b>	<b>0.466</b>	0.341	0.403	<b>0.633</b>	0.624	0.628

the best choice for  $T \rightarrow I$  retrieval task. This behavior is also confirmed by the retrieval results in terms of ROUGE-L scores. For the  $I \rightarrow T$  retrieval task, one can notice that with the TFF strategy the proposed method achieves the highest retrieval scores across all the metrics. As an example, with the TFF strategy the proposed method achieves a METEOR and ROUGE-L score of 0.332 and 0.523, respectively overcoming the utilization of the GFF: strategies by approximately 3%. When analyzing the average retrieval scores across the two tasks, one can notice that with the TFF strategy once again the proposed method achieves the highest retrieval results across all the metrics significantly surpassing the GFF strategies. These results highlights once again the effectiveness of the TFF strategy in modeling the semantic content of bitemporal images. As a results, the utilization of the TFF strategy in the proposed text-ITSR method yields the highest results across the two tasks over all the metrics. Among the GFF strategies, the utilization of the GFF: Subtraction strategy shows better performances compared to the utilization of the GFF: Concatenation one across the tasks.

2) *Change query set scenario*: Similar to the previous scenario, in the change query set scenario, with the TFF strategy the proposed method achieves the highest results on average across the two tasks. For instance, for the  $T \rightarrow I$

retrieval task utilizing the TFF strategy to model the semantic content of the bitemporal images the proposed method achieves a BLEU-4 score of 0.224 surpassing the utilization of the GFF: Concatenation and the GFF: Subtraction strategies by approximately 6% and 2%, respectively. One can notice a similar behavior when looking at the achieved scores in terms of METEOR and ROUGE-L. These results confirms the capability of TFF strategy in effectively modeling the semantic changes over bitemporal images and thus allowing the proposed method to better align bitemporal images and text sentences associated with change and, achieving the highest retrieval accuracy in the  $T \rightarrow I$  retrieval task. For  $I \rightarrow T$  retrieval task, one can notice that the highest retrieval results by the proposed method are achieved when the GFF: Concatenation strategy is used to model the semantic content of the bitemporal images. As an example, one can notice that with the GFF: Concatenation strategy the proposed method achieves a BLEU-4 score of 0.208 surpassing the utilization of the TFF and GFF: Subtraction strategies by approximately 1% and 2%, respectively. One can notice that this improvement is reflected also when looking and the retrieval results in terms of METEOR and ROUGE-L. However, when looking at the average scores across the two tasks, the integration of the TFF strategy into the proposed method achieves the

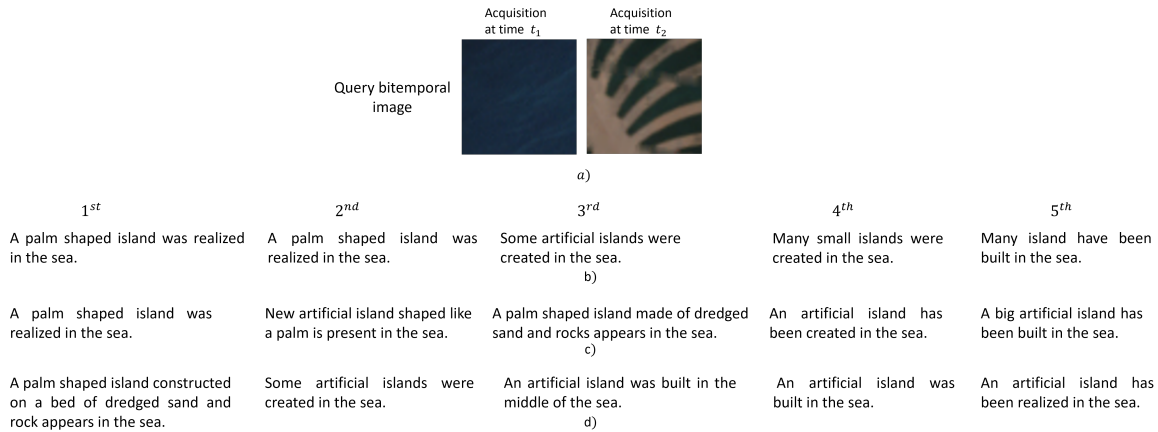


Fig. 6:  $I \rightarrow T$  retrieval example for Dubai CCD. a) query bitemporal images and retrieved text sentences by the proposed cross-modal text-ITSR method when the: b) GFF: Concatenation, c) GFF: Subtraction and d) TFF strategies are used to model the semantic content of bitemporal images.

highest retrieval results making it the best choice to model the semantic content of bitemporal images associated with change. As an example, the integration of the TFF strategy provides an improvement over the GFF strategies of around 2% in all the considered metrics. These results once again emphasize the robustness of the TFF strategies in modeling changes over bitemporal images. Thus, when integrated into the proposed text-ITSR method allows for a better cross-modal text-image alignment compared to the GFF strategies.

3) *No-change query set scenario*: In this scenario, we can see a similar trend as in the full query set scenario where for the  $T \rightarrow I$  retrieval task, the integration of the GFF: Subtraction strategy provides the highest retrieval results, whereas for the  $I \rightarrow T$  retrieval task the integration of the TFF strategy provides the highest retrieval results. As an example, for the  $T \rightarrow I$  retrieval task, the proposed text-ITSR method achieves a BLEU-4 score of 0.419 with the GFF: Subtraction strategy, surpassing integration of the TFF and GFF: Concatenation strategies by approximately 3% and 12%, respectively. For the  $I \rightarrow T$  retrieval task one can see that with the TFF strategy the proposed method attains a BLEU-4 score of 0.378, outperforming the integration of the GFF: Subtraction and Concatenation strategies by approximately 10% and 14%, respectively. By analyzing Table II, one can notice that using the TFF strategy in the proposed method results in obtaining more more balanced scores across the two tasks. As an example, with the TFF strategy the proposed method attains a BLEU-4 score of 0.38 which is approximately 10% and 6% higher compared to the one achieved when GFF: Concatenation and GFF: Sbtraction is integrated, respectively. This shows that the TFF strategy is more robust compared to the other two strategies in modeling the semantic content over bitemporal images. As a result, its integration in the proposed text-ITSR method leads to better and more balanced cross-modal retrieval performances.

Figure 5 shows a  $T \rightarrow I$  retrieval example where the query text is: "One big road appeared in the desert." and the bitemporal images retrieved by the proposed cross-modal text-ITSR method using the GFF: Concatenation [Fig. 5 b)], GFF:

Subtraction [see Fig. 5 c)] and TFF [see Fig. 5 d)] strategies to model the semantic content of the bitemporal images. One can notice that almost all the retrieved bitemporal images correctly depict changes involving the appearance of a road in the desert. By analyzing the figure further, the retrieved images obtained when using the TFF strategy in the proposed method exhibit a stronger alignment with the query text compared to those retrieved when using the GFF strategies. Specifically, the four retrieved bitemporal images by the proposed method when utilizing the TFF strategy depict exactly the appearance of a road in a desert. On the other hand, when utilizing the GFF strategies some inaccuracies are observed in the retrieved images by the proposed method. For instance, the 3<sup>rd</sup> and 5<sup>th</sup> retrieved images by the proposed method when utilizing the GFF strategies do not align with the query text sentence.

Figure 6 shows an  $I \rightarrow T$  retrieval example, where one of the reference descriptions of the query bitemporal images [Fig. 6 a) ] is "A palm shaped island constructed on a bed of dredged sand and rock appears in the sea." and the text sentences retrieved by the proposed cross-modal text-ITSR method using the GFF: Concatenation [Fig. 6 b)], GFF: Subtraction [see Fig. 6 c)] and TFF [see Fig. 6 d)] strategies. Notably, all retrieved descriptions semantically capture the change between the two image acquisitions that is "the formation of an island in the sea". Furthermore, some of the retrieved descriptions include important attributes such as the shape and the size of the created island.

## VI. CONCLUSION

In this paper, as a first time in RS we have addressed the text-ITSR which refers to the retrieval of image time series using text sentences as queries and vice versa. In particular, we proposed a self-supervised text-ITSR method focusing on pairs of images (i.e., bitemporal images). The proposed method is composed of two main components: 1) modality-specific encoders to extract discriminative features from bitemporal images and text sentences and 2) modality-specific projection heads to align textual and image features in a common embedding space using contrastive learning.

To model temporal information at the feature level, we have introduced two fusion strategies: i) the global feature fusion (GFF) strategy, which combines global feature using two simple yet effective operators, feature concatenation and feature subtraction; and ii) transformer-based feature fusion (TFF) strategy that leverages the transformer architecture for fine-grained information. In the experiments, we evaluated our method by using two datasets under two tasks: i) RS image time series retrieval with a text sentence as query; and ii) sentence retrieval with a RS image time series as query. The experimental results show the effectiveness of the proposed text-ITSR method in accurately retrieving bitemporal images given a query text sentence and vice versa. Among the fusion strategies, TFF is the most effective strategy for modeling temporal information within bitemporal images, leading to more accurate retrieval results across modalities compared to GFF strategies. This is more visible in the cases in which the queries (text sentences or bitemporal images) represent changes. This improved performance is attributed to the specific design of the TFF strategy to capture the changes within the bitemporal images.

We would like to note that although this work focuses on text-ITSR problems, the proposed architecture and training strategy have the potential to serve as a foundation model when pre-trained in larger datasets. Through fine-tuning applied using annotated image time series, the pre-trained modality-specific encoders could support various downstream tasks related to the analysis of image time series. As a future development of our work, we plan to investigate the effectiveness of the proposed method for tasks such as change captioning and change related questioning answering. In addition, we plan to test the proposed method in the context of retrieving long-term changes.

## REFERENCES

- [1] F. Bovolo, B. Demir, and L. Bruzzone, "A cluster-based approach to content based time series retrieval (cbtsr)," in *2015 IEEE International Geoscience and Remote Sensing Symposium (IGARSS)*, pp. 2793–2796, 2015.
- [2] O. Vuran, O. Akcin, M. Ravanbakhsh, B. Sankur, and B. Demir, "Deep learning driven content-based image time-series retrieval in remote sensing archives," in *IGARSS 2022 - 2022 IEEE International Geoscience and Remote Sensing Symposium*, pp. 1940–1943, 2022.
- [3] C. Ma, W. Xia, F. Chen, J. Liu, Q. Dai, L. Jiang, J. Duan, and W. Liu, "A content-based remote sensing image change information retrieval model," *ISPRS International Journal of Geo-Information*, vol. 6, no. 10, p. 310, 2017.
- [4] X. X. Zhu, D. Tuia, L. Mou, G.-S. Xia, L. Zhang, F. Xu, and F. Fraundorfer, "Deep learning in remote sensing: A comprehensive review and list of resources," *IEEE Geoscience and Remote Sensing Magazine*, vol. 5, no. 4, pp. 8–36, 2017.
- [5] D. Tuia, K. Schindler, B. Demir, X. X. Zhu, M. Kochupillai, S. Džeroski, J. N. van Rijn, H. H. Hoos, F. Del Frate, M. Datcu, V. Markl, B. Le Saux, R. Schneider, and G. Camps-Valls, "Artificial intelligence to advance earth observation: A review of models, recent trends, and pathways forward," *IEEE Geoscience and Remote Sensing Magazine*, pp. 2–25, 2024.
- [6] S. Saha, F. Bovolo, and L. Bruzzone, "Unsupervised deep change vector analysis for multiple-change detection in vhr images," *IEEE Transactions on Geoscience and Remote Sensing*, vol. 57, no. 6, pp. 3677–3693, 2019.
- [7] G. Hoxha, F. Melgani, and B. Demir, "Toward remote sensing image retrieval under a deep image captioning perspective," *IEEE Journal of Selected Topics in Applied Earth Observations and Remote Sensing*, vol. 13, pp. 4462–4475, 2020.
- [8] T. Abdullah, Y. Bazi, M. M. Al Rahhal, M. L. Mekhalif, L. Rangarajan, and M. Zuair, "Textrs: Deep bidirectional triplet network for matching text to remote sensing images," *Remote Sensing*, vol. 12, no. 3, 2020.
- [9] M. M. A. Rahhal, Y. Bazi, T. Abdullah, M. L. Mekhalif, and M. Zuair, "Deep unsupervised embedding for remote sensing image retrieval using textual cues," *Applied Sciences*, vol. 10, no. 24, p. 8931, 2020.
- [10] Q. Cheng, Y. Zhou, P. Fu, Y. Xu, and L. Zhang, "A deep semantic alignment network for the cross-modal image-text retrieval in remote sensing," *IEEE Journal of Selected Topics in Applied Earth Observations and Remote Sensing*, vol. 14, pp. 4284–4297, 2021.
- [11] G. Mikriukov, M. Ravanbakhsh, and B. Demir, "Deep unsupervised contrastive hashing for large-scale cross-modal text-image retrieval in remote sensing," *arXiv preprint arXiv:2201.08125*, 2022.
- [12] M. M. A. Rahhal, Y. Bazi, N. A. Alsharif, L. Bashmal, N. Alajlan, and F. Melgani, "Multilanguage transformer for improved text to remote sensing image retrieval," *IEEE Journal of Selected Topics in Applied Earth Observations and Remote Sensing*, vol. 15, pp. 9115–9126, 2022.
- [13] G. Mikriukov, M. Ravanbakhsh, and B. Demir, "Unsupervised contrastive hashing for cross-modal retrieval in remote sensing," in *ICASSP 2022 - 2022 IEEE International Conference on Acoustics, Speech and Signal Processing (ICASSP)*, pp. 4463–4467, 2022.
- [14] L. Mi, X. Dai, J. Castillo-Navarro, and D. Tuia, "Knowledge-aware text-image retrieval for remote sensing images," *IEEE Transactions on Geoscience and Remote Sensing*, vol. 62, pp. 1–13, 2024.
- [15] T. Sun, C. Zheng, X. Li, Y. Gao, J. Nie, L. Huang, and Z. Wei, "Strong and weak prompt engineering for remote sensing image-text cross-modal retrieval," *IEEE Journal of Selected Topics in Applied Earth Observations and Remote Sensing*, pp. 1–12, 2025.
- [16] S. Hochreiter and J. Schmidhuber, "Long Short-Term Memory," *Neural Computation*, vol. 9, pp. 1735–1780, 11 1997.
- [17] R. Hadsell, S. Chopra, and Y. LeCun, "Dimensionality reduction by learning an invariant mapping," in *2006 IEEE Computer Society Conference on Computer Vision and Pattern Recognition (CVPR'06)*, vol. 2, pp. 1735–1742, 2006.
- [18] E. Hoffer and N. Ailon, "Deep metric learning using triplet network," in *Similarity-Based Pattern Recognition* (A. Feragen, M. Pelillo, and M. Loog, eds.), (Cham), pp. 84–92, Springer International Publishing, 2015.
- [19] Z. Yuan, W. Zhang, K. Fu, X. Li, C. Deng, H. Wang, and X. Sun, "Exploring a fine-grained multiscale method for cross-modal remote sensing image retrieval," *IEEE Transactions on Geoscience and Remote Sensing*, vol. 60, pp. 1–19, 2022.
- [20] Z. Yuan, W. Zhang, X. Rong, X. Li, J. Chen, H. Wang, K. Fu, and X. Sun, "A lightweight multi-scale crossmodal text-image retrieval method in remote sensing," *IEEE Transactions on Geoscience and Remote Sensing*, vol. 60, pp. 1–19, 2022.
- [21] Z. Yuan, W. Zhang, C. Tian, X. Rong, Z. Zhang, H. Wang, K. Fu, and X. Sun, "Remote sensing cross-modal text-image retrieval based on global and local information," *IEEE Transactions on Geoscience and Remote Sensing*, vol. 60, pp. 1–16, 2022.
- [22] J. Deng, W. Dong, R. Socher, L.-J. Li, K. Li, and L. Fei-Fei, "Imagenet: A large-scale hierarchical image database," in *2009 IEEE Conference on Computer Vision and Pattern Recognition*, pp. 248–255, 2009.
- [23] A. Vaswani, "Attention is all you need," *Advances in Neural Information Processing Systems*, 2017.
- [24] Y. Yuan, Y. Zhan, and Z. Xiong, "Parameter-efficient transfer learning for remote sensing image-text retrieval," *IEEE Transactions on Geoscience and Remote Sensing*, vol. 61, pp. 1–14, 2023.
- [25] Y. Chen, J. Huang, S. Xiong, and X. Lu, "Integrating multisubspace joint learning with multilevel guidance for cross-modal retrieval of remote sensing images," *IEEE Transactions on Geoscience and Remote Sensing*, vol. 62, pp. 1–17, 2024.
- [26] G. Hu, Z. Wen, Y. Lv, J. Zhang, and Q. Wu, "Global-local information soft-alignment for cross-modal remote-sensing image-text retrieval," *IEEE Transactions on Geoscience and Remote Sensing*, vol. 62, pp. 1–15, 2024.
- [27] D. Wu, H. Li, Y. Hou, C. Xu, G. Cheng, L. Guo, and H. Liu, "Spatial-channel attention transformer with pseudo regions for remote sensing image-text retrieval," *IEEE Transactions on Geoscience and Remote Sensing*, vol. 62, pp. 1–15, 2024.
- [28] Z. Zhao, X. Miao, C. He, J. Hu, B. Min, Y. Gao, Y. Liu, and K. Phark-suwan, "Masking-based cross-modal remote sensing image-text retrieval via dynamic contrastive learning," *IEEE Transactions on Geoscience and Remote Sensing*, vol. 62, pp. 1–15, 2024.
- [29] Y. Chen, J. Huang, S. Xiong, and X. Lu, "Integrating multisubspace joint learning with multilevel guidance for cross-modal retrieval of remote

- sensing images,” *IEEE Transactions on Geoscience and Remote Sensing*, vol. 62, pp. 1–17, 2024.
- [30] L. Bashmal, S. M. A. Mehmadi, Y. Bazi, M. M. A. Rahhal, and M. Zuair, “Text-to-event retrieval in aerial videos,” *IEEE Geoscience and Remote Sensing Letters*, vol. 21, pp. 1–5, 2024.
- [31] A. Radford, J. W. Kim, C. Hallacy, A. Ramesh, G. Goh, S. Agarwal, G. Sastry, A. Askell, P. Mishkin, J. Clark, G. Krueger, and I. Sutskever, “Learning transferable visual models from natural language supervision,” in *International Conference on Machine Learning*, 2021.
- [32] R. Arandjelovic, P. Gronat, A. Torii, T. Pajdla, and J. Sivic, “Netvlad: Cnn architecture for weakly supervised place recognition,” in *Proceedings of the IEEE conference on computer vision and pattern recognition*, pp. 5297–5307, 2016.
- [33] J. Devlin, M. Chang, K. Lee, and K. Toutanova, “BERT: pre-training of deep bidirectional transformers for language understanding,” in *Proceedings of the 2019 Conference of the North American Chapter of the Association for Computational Linguistics: Human Language Technologies, NAACL-HLT 2019, Minneapolis, MN, USA, June 2-7, 2019, Volume 1 (Long and Short Papers)* (J. Burstein, C. Doran, and T. Solorio, eds.), pp. 4171–4186, Association for Computational Linguistics, 2019.
- [34] A. Dosovitskiy, L. Beyer, A. Kolesnikov, D. Weissenborn, X. Zhai, T. Unterthiner, M. Dehghani, M. Minderer, G. Heigold, S. Gelly, J. Uszkoreit, and N. Houlsby, “An image is worth 16x16 words: Transformers for image recognition at scale,” *ArXiv*, vol. abs/2010.11929, 2020.
- [35] C. Liu, R. Zhao, H. Chen, Z. Zou, and Z. Shi, “Remote sensing image change captioning with dual-branch transformers: A new method and a large scale dataset,” *IEEE Transactions on Geoscience and Remote Sensing*, vol. 60, pp. 1–20, 2022.
- [36] K. Sohn, “Improved deep metric learning with multi-class n-pair loss objective,” *Advances in neural information processing systems*, vol. 29, 2016.
- [37] G. Hoxha, S. Chouaf, F. Melgani, and Y. Smara, “Change captioning: A new paradigm for multitemporal remote sensing image analysis,” *IEEE Transactions on Geoscience and Remote Sensing*, vol. 60, pp. 1–14, 2022.
- [38] K. Papineni, S. Roukos, T. Ward, and W.-J. Zhu, “Bleu: a method for automatic evaluation of machine translation,” in *Proceedings of the 40th Annual Meeting on Association for Computational Linguistics, ACL ’02, (USA)*, p. 311–318, Association for Computational Linguistics, 2002.
- [39] S. Banerjee and A. Lavie, “METEOR: An automatic metric for MT evaluation with improved correlation with human judgments,” in *Proceedings of the ACL Workshop on Intrinsic and Extrinsic Evaluation Measures for Machine Translation and/or Summarization* (J. Goldstein, A. Lavie, C.-Y. Lin, and C. Voss, eds.), (Ann Arbor, Michigan), pp. 65–72, Association for Computational Linguistics, June 2005.
- [40] C.-Y. Lin, “ROUGE: A package for automatic evaluation of summaries,” in *Text Summarization Branches Out*, (Barcelona, Spain), pp. 74–81, Association for Computational Linguistics, July 2004.